Transcriptomic Profiling of Resistant and Susceptible Chickens (*Gallus gallus*) Identifies Potential Cellular Processes Underlying Resistance to Avian Leukosis Virus Subgroup J

Abdulazeez Giwa[1], Maridiyat Odele[1], Oluwafunmito Ishola[1], Oluwabusayo Roleola[1], Zainab Abdulrahman-Giwa[2]

[1]*Department of Zoology and Environmental Biology, Faculty of Science, Lagos State University, P.M.B. 0001, LASU Post Office, Lagos-Badagry Expressway, Ojo, Lagos*

[2]*Department of Basic Science, Eko University of Medicine and Health Sciences, Km 28, Lagos-Badagry Expressway, Ojo, Lagos 102101, Lagos*

Keywords: *ALV-J, transcriptomics, RNA-Seq, chickens, biomarkers.*

Abstract. *The study aimed to investigate transcriptomic mechanisms underlying natural resistance to avian leukosis virus subgroup J (ALV-J) in chickens by comparing resistant and susceptible individuals using high-throughput RNA sequencing. The PRJNA685043 RNA-Seq dataset available on the FAANG data portal was used for analyses. The gene expression profiles of chicken liver tissues from ALV-J-resistant and ALV-J-susceptible birds (N = 6; 3 resistant and 3 susceptible) were analyzed to identify differentially expressed genes (DEGs), differential transcript usage (DTU), and associated molecular pathways that may contribute to viral resistance. Transcript quantification was performed using kallisto, followed by differential gene expression (DGE) analysis with DESeq2 and DTU evaluation using a combined DRIMSeq–DEXSeq–stageR workflow. Functional characterization and interaction profiling were conducted using STRING and additional regulatory analyses. The analysis identified 36 significant DEGs, including 32 upregulated and 4 downregulated genes in resistant chickens. Key genes were associated with mitochondrial regulation, calcium signaling, DNA damage response, and suppression of tumorigenesis. DTU analysis revealed 22 genes exhibiting significant isoform switching, suggesting alternative splicing as an additional regulatory layer. Interaction network assessment highlighted limited but meaningful relationships among DEGs and DTU genes, indicating that multiple independent pathways may contribute collectively to resistance.*

Introduction

Avian leukosis virus subgroup J (ALV-J) remains one of the most economically important viral pathogens affecting commercial poultry flocks worldwide. The virus causes myelocytomas, immunosuppression, reduced growth and increased mortality, posing a serious threat to intensive chicken production systems (Wessi, 2011; Payne and Nair, 2012). ALV-J is an oncogenic retrovirus inducing tumor formation in chickens via genome insertion thereby dysregulating oncogenes and tumor suppressor genes in chickens (Justice et al., 2015; Ren et al., 2018). Despite concerted control efforts, ALV-J persists in many regions because management measures and culling alone are insufficient to protect genetically susceptible birds (Nakamura and Nair, 2014).

Transcriptomic studies have shown that ALV-J infection perturbs host gene expression and cellular signaling, pointing to host-response variation as a determinant of disease outcome (Raun et al., 2004; Han et al., 2015). These investigations have reported dysregulation of immune pathways, metabolic functions and cell-cycle programs following infection, and recent work highlights the additional role of alternative splicing and isoform-level regulation in modulating antiviral responses (Zhang et al., 2025). Such observations imply that differences in global transcriptional responses could underlie why some birds resist infection while others develop severe disease.

While several studies have catalogued host genes affected by ALV-J, far fewer have compared the constitutive transcriptomic architecture that distinguishes inherently resistant lines from susceptible ones. Identifying these baseline differences is critical for discovering robust biomarkers and molecular pathways that can be used in selective-breeding strategies to reduce flock susceptibility (Mo et al., 2022). A focused comparison of resistant and susceptible chickens at the transcriptome and isoform levels therefore provides a powerful route to reveal candidate mechanisms of natural resistance.

Here, we performed an integrated analysis combining differential gene expression (DGE), differential transcript usage (DTU), and protein–protein interaction mapping to compare liver transcriptomes from genetically resistant and susceptible chickens. Our goal was to detect consistent molecular signatures associated with resistance and to nominate genes and pathways for follow-up functional validation and application in breeding programs.

Corresponding author: abdulazeez.giwa@lasu.edu.ng

Materials and methods

Data collection

The PRJNA685043 dataset (GSE163135) was obtained from the FAANG data portal at https://data.faang.org/dataset/PRJNA685043. The PRJNA685043 dataset is an RNA-Seq dataset of liver tissue of ALV-J resistant and ALV-J susceptible chickens consisting of three samples each. These samples were sequenced on the Illumina HiSeq 4000 platform. The sequencing files were paired-end, i.e., both ends of DNA fragment sequenced, and were in fastq.gz format. Sample collection, preparation, sequencing are as outlined in Yan et al. (2021).

Quality control of data

Quality of the sequencing FASTQ files was assessed using FastQC tool (v0.12.1). FastQC provides a simple way to perform quality control checks on raw sequence data from high throughput sequencing pipelines. It analyzes the sequencing files so as to flag issues the analyst should be aware of before further analysis. A report for each analyzed sequencing file is generated including summary graphs of multiple quality indicators such as base quality, overrepresented sequences, adapter content etc. After FastQC, reads were trimmed and adapters removed using Trimmomatic (v0.39) (Bolger et al., 2014).

The command used to remove adapters, leading and trailing low-quality bases, and to drop reads below the specified length was: "java -jar trimmomatic-0.39.jar PE -phred33 {sequence-file1-forward.fastq.gz} {sequence-file1-reverse.fastq.gz} {sequence-file1-forward_paired.fastq.gz} {sequence-file1-forward_unpaired.fastq.gz} {sequence-file1-reverse_paired.fastq.gz} {sequence-file1-reverse_unpaired.fastq.gz} ILLUMINACLIP:TruSeq3-PE.fa:2:30:10 LEADING:3 TRAILING:3 SLIDINGWINDOW:4:15 MINLEN:36". ILLUMINACLIP:TruSeq3-PE.fa:2:30:10 was used to remove adapters, LEADING:3 was used to remove leading low quality or N bases (below quality three), TRAILING:3 was used to remove trailing low quality or N bases (below quality three), and MINLEN:36 was used to drop reads below 36 bases long. To ensure all sequence reads passed basic quality statistics, the trimmed and paired sequence files were checked using FastQC. The trimmed files were then used for transcript quantification via pseudoalignment.

Transcript abundance quantification

Quantification of transcript abundance from the RNA-Seq reads (the trimmed paired files) of the samples was performed using kallisto (version 0.46.1) via the pseudo alignment method (Bray et al., 2016). Firstly, a transcriptome index was created using the *Gallus gallus* transcriptome (cDNA) (release 113) downloaded from Ensembl database (https://www.ensembl.org/index.html). The corresponding GTF annotation file was also downloaded from the Ensembl database for use in downstream DTU analysis. Abundance quantification of transcripts was thereafter performed for the trimmed-paired sequencing files and the quantification outputs exported to specified folders for downstream use.

Differential gene expression

The transcript abundance estimates quantified were imported into R (version 4.4.1) using tximport package (Soneson et al., 2015). These estimates were imported for use with Differential Gene Expression (DGE) methods using the DESeqDataSetFromTximport function from DESeq2 package (Love et al., 2014). Genes with low expression across samples were filtered to reduce noise. DGE analysis was performed between the ALV-J-resistant and ALV-J-susceptible groups using DESeq2. An adjusted P value < 0.05 and a lfcThreshold of 0.3 were set in the DGE analysis to identify differentially expressed genes (DEGs). Heatmap plotting and sample clustering using the DEGs was thereafter performed with the pheatmap package.

Differential transcript usage

Differential transcript usage (DTU) analysis was performed following the workflow described in Love et al. (2018). The transcript abundance estimates quantified were imported into R using tximport package (Soneson et al., 2015). The data object was filtered to remove low expressed transcripts that may affect parameter estimation and increase fitting speed (Love et al., 2018). The filtering criteria included retaining a transcript with a count of at least two in at least three samples, having a relative abundance proportion of at least 0.1 in at least two samples, and the total count of the corresponding gene is at least two in all six samples. The filtering retained 2733 genes and 5981 transcripts. Thereafter, DRIMSeq (Nowicka and Robinson, 2016), DEXSeq (Anders et al., 2012; Reyes et al., 2013) and stageR (Van den Berge et al., 2018) packages were used for the DTU analysis. An alpha (α) value of 0.05 and adjusted P value < 0.05 were used as thresholds for the identification of genes with significant differentially used transcripts.

Interaction and transcriptional regulatory analysis

Protein-protein interaction analysis of the DEGs and DTU genes identified was performed with STRING (version 12.0) (Szklarczyk et al., 2021). TRRUST (version 2) (Han et al., 2018), was used to perform transcriptional regulatory analysis to reveal the transcription factors regulating the identified DEGs and DTU genes. The inputs into the TRRUST database were the list of DEGs and the DTU genes with the expected output being a tabular list of transcription factors regulating the input genes.

Results

Differential gene expression analysis

RNA-seq profiling generated expression data for 17 068 annotated genes across all samples. Comparative analysis of ALV-J–resistant and ALV-J–susceptible chickens identified a distinct set of 36 differentially expressed genes (DEGs), consisting of both annotated genes and several uncharacterized loci. These DEGs are summarized in Table 1.

Unsupervised hierarchical clustering using the complete DEG set clearly separated resistant birds from susceptible ones, reflecting substantial

Table 1. Information on the DEGs in ALV-J resistant samples compared with ALV-J susceptible samples. Shown are gene symbol, gene names, log2FC, p-adjusted value and status. Genes without gene names are novel genes with no gene name and symbol assigned on the Ensembl database

Symbol	Gene Name	Log2FC	p-adj	Status
ENSGALG00010003287 (novel gene)		10.454	4.09e-06	Up
MTMR7	myotubularin related protein 7	10.103	2.29e-06	Up
TMEM104	transmembrane protein 104	9.307	0.00054	Up
SAMD8	Sterile alpha motif domain containing 8	9.228	0.00511	Up
CINP	cyclin dependent kinase 2 interacting protein	9.135	0.00788	Up
ADRB1	adrenoceptor beta 1	9.069	0.00788	Up
SSH2	slingshot protein phosphatase 2	9.044	0.00788	Up
ZNF341	zinc finger protein 341	8.861	0.0065	Up
ZNF362	zinc finger protein 362	8.849	0.00788	Up
IFT81	intraflagellar transport 81	8.789	0.00788	Up
TRPV3	transient receptor potential cation channel subfamily V member 3	8.719	0.00832	Up
CASR	calcium sensing receptor	8.715	0.02399	Up
LRAT	lecithin retinol acyltransferase	8.587	0.01936	Up
BRAT1	BRCA1 associated ATM activator 1	8.577	0.03562	Up
ENSGALG00010023766 (novel gene)		8.574	0.02358	Up
CCR8	C-C motif chemokine receptor 8	8.517	0.03714	Up
EARS2	glutamyl-tRNA synthetase 2, mitochondrial	8.506	0.02358	Up
PIGQ	phosphatidylinositol glycan anchor biosynthesis class Q	8.476	0.02871	Up
MGME1	mitochondrial genome maintenance exonuclease 1	8.475	0.02523	Up
SMDT1	single-pass membrane protein with aspartate rich tail 1	8.475	0.04329	Up
CHEK1	checkpoint kinase 1	8.463	0.02399	Up
WDHD1	WD repeat and HMG-box DNA binding protein 1	8.4532	0.03956	Up
GAB3	GRB2 associated binding protein 3	8.388	0.03562	Up
SLC25A43	solute carrier family 25member 43	8.117	0.00511	Up
DFFB	DNA fragmentation factor subunit beta	7.972	0.00054	Up
ENSGALG00010012307 (Novel gene)		7.896	6.84e-05	Up
CKB	creatine kinase B	7.833	0.02309	Up
CLEC14A	C-type lectin domain containing 14A	6.393	0.00788	Up
TMOD2	tropomodulin 2	8.379	0.03714	Up
ENSGALG00010015655 (novel gene)		8.319	0.04991	Up
SNX11	sorting nexin 11	8.319	0.04692	Up
NEK10	NIMA related kinase 10	6.136	0.00788	Up
CYP1A2	cytochrome P450, family 1, subfamily A, polypeptide 2	-1.895	0.00071	Down
SSPN	Sarcospan	-3.85	0.02309	Down
CHRM3	cholinergic receptor muscarinic 3	-4.201	0.02358	Down
GRIN2A	glutamate ionotropic receptor NMDA type subunit 2A	-8.377	3.21e-05	Down

transcriptomic divergence between the phenotypes. This grouping pattern is illustrated in Fig. 1, where resistant samples consistently formed a distinct cluster relative to susceptible individuals.

Differential transcript usage analysis

Differential transcript usage (DTU) analysis was conducted on 13 566 expressed transcripts to identify isoform-level regulatory differences between the two groups. Several genes displayed significant shifts in transcript proportions, indicating that isoform regulation contributes to phenotypic variation in ALV-J response. Examples of transcripts with notable usage changes include isoforms of *MAGI1, FGFR3, RCN1, AKAP9, DYRK1A,* and *COQ8A*, with representative DTU plots shown in Figs. 2–6.

The presence of DTU events in multiple functionally relevant genes suggests that alternative splicing may play an important role in modulating antiviral or stress-response functions in resistant chickens.

Interaction and transcriptional regulatory network analysis

Integration of the DEGs and DTU-associated genes into a protein–protein interaction (PPI) framework revealed a condensed set of interconnected molecules forming key regulatory clusters. Notable nodes included *AKAP9, FGFR3, EML4, ARID1B, DYRK1A*, and *VPS26C*, many of which participate in cellular signaling, transcriptional regulation, or structural maintenance.

A comprehensive PPI map is presented in Fig. 7, highlighting the central interacting genes while omitting non-connected nodes for clarity. This network emphasizes the biological coherence of the transcriptomic signals identified through both DGE and DTU analyses.

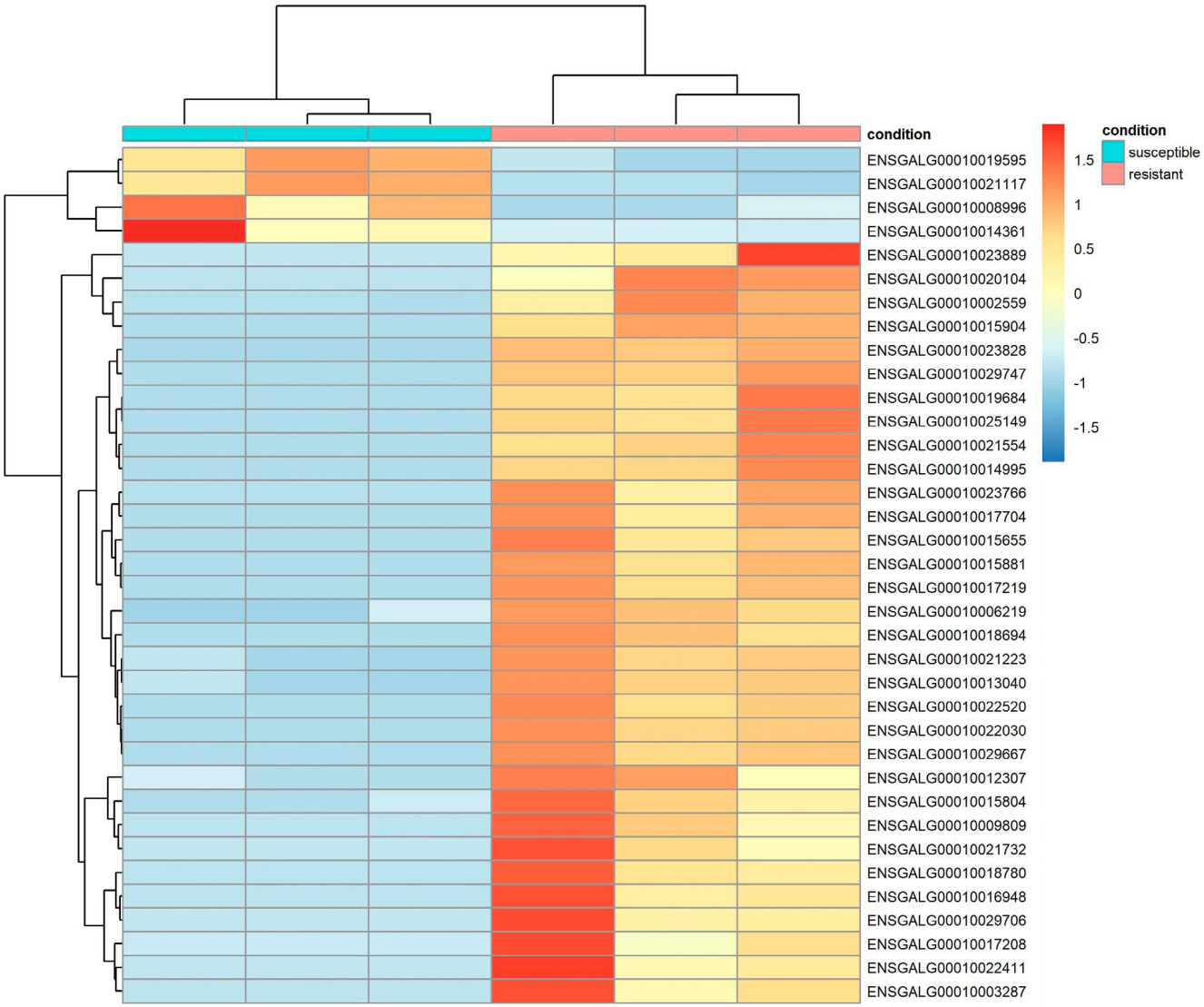

Fig. 1. Heatmap and clustering of the susceptibility and resistance samples by the identified differentially expressed genes

Table 2. Information on the identified DTU genes (with adjusted *P* value < 0.05). Included are the gene symbols, gene names, transcript IDs and *P* adjusted value (to 3 decimal places)

Symbol	Gene name	Transcript id	*P* adj
DSCR3	VPS26 endosomal protein sorting factor C	ENSGALT00010031585	0.038
SPATS2L	spermatosis associated serine rich 2 like	ENSGALT00010058702	0.038
SPCS3	signal peptidase complex subunit 3	ENSGALT00010007997	0.046
		ENSGALT00010008013	0.046
ARID1B	AT-rich interaction domain 1B	ENSGALT00010009548	0.006
		ENSGALT00010009555	0.006
AKAP9	A-kinase anchoring protein 9	ENSGALT00010011356	0.029
		ENSGALT00010011383	0.029
PROSER2	proline and serine rich 2	ENSGALT00010013650	0.024
		ENSGALT00010013656	0.024
MCTS1	MCTS1, re-initiation and release factor	ENSGALT00010029418	0.047
		ENSGALT00010029420	0.047
SCAMP1	secretory carrier membrane protein 1	ENSGALT00010030297	0.033
		ENSGALT00010029420	0.033
DYRK1A	dual specificity tyrosine phosphorylation regulated kinase 1A	ENSGALT00010031626	0.007
		ENSGALT00010031632	0.007
MRPS9	mitochondrial ribosomal protein S9	ENSGALT00010031727	0.048
		ENSGALT00010031729	0.048
MAN1A1	mannosidase alpha class 1A member 1	ENSGALT00010036052	0.018
		ENSGALT00010036068	0.018
FGFR3	fibroblast growth factor receptor 3	ENSGALT00010040904	0.046
		ENSGALT00010040908	0.046
COQ8A	coenzyme Q8A	ENSGALT00010043588	0.013
		ENSGALT00010043592	0.013
EML4	EMAP like 4	ENSGALT00010045339	0.037
		ENSGALT00010045344	0.037
SUCLG2	succinate-CoA ligase GDP-forming beta subunit	ENSGALT00010047717	0.034
		ENSGALT00010047749	0.034
MAGI1	membrane associated guanylate kinase 1	ENSGALT00010048939	0.021
		ENSGALT00010048945	0.021
RCN1	reticulocalbin 1	ENSGALT00010057659	0.009
		ENSGALT00010057669	0.009
GABARAPL1	GABA type A receptor associated protein like 1	ENSGALT00010058708	0.033
		ENSGALT00010058714	0.033
HIC2	HIC ZBTB transcriptional repressor 2	ENSGALT00010059216	0.047
		ENSGALT00010059236	0.047
RIT1	Ras like without CAAX 1	ENSGALT00010068899	0.049
		ENSGALT00010068900	0.049
SUGP1	SURP and G-patch domain containing 1	ENSGALT00010069080	0.049
		ENSGALT00010069081	0.049
CASP1	caspase 1	ENSGALT00010071575	0.033
		ENSGALT00010071577	0.033

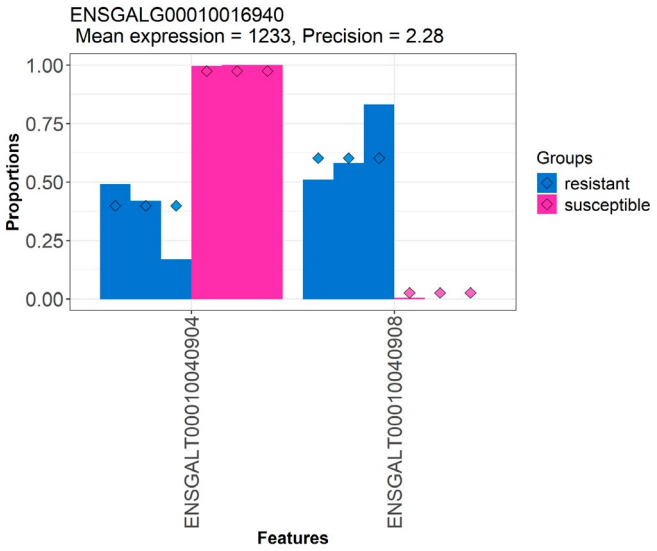

Fig. 2. Plot of the estimated transcript proportions for ENSGALG00010016940 (*FGFR3*)

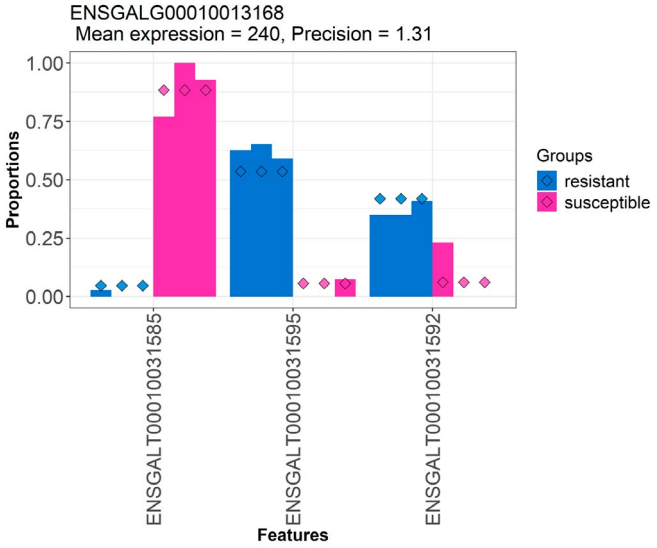

Fig. 3. Plot of the estimated transcript proportions for ENSGALG00010023668 (*RCN1*)

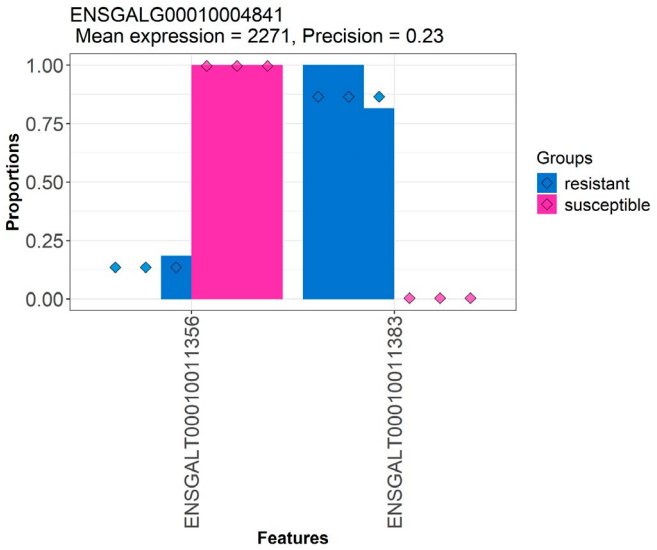

Fig. 4. Plot of the estimated transcript proportions for ENSGALG00010004841 (*AKAP9*)

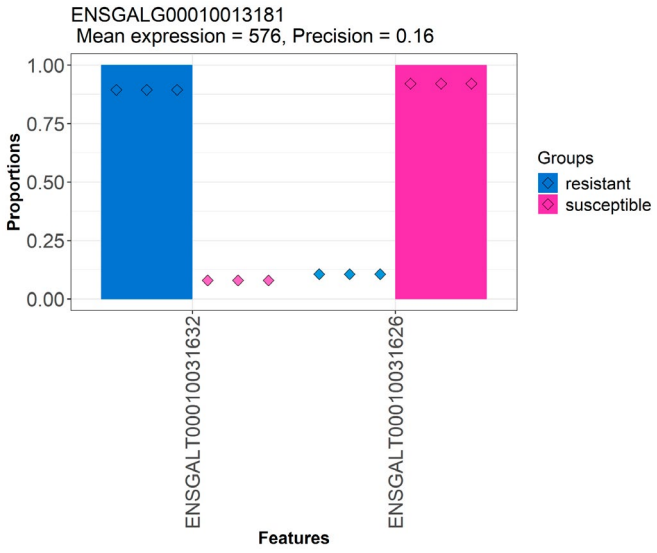

Fig. 5. Plot of the estimated transcript proportions for ENSGALG00010013181 (*DYRK1A*)

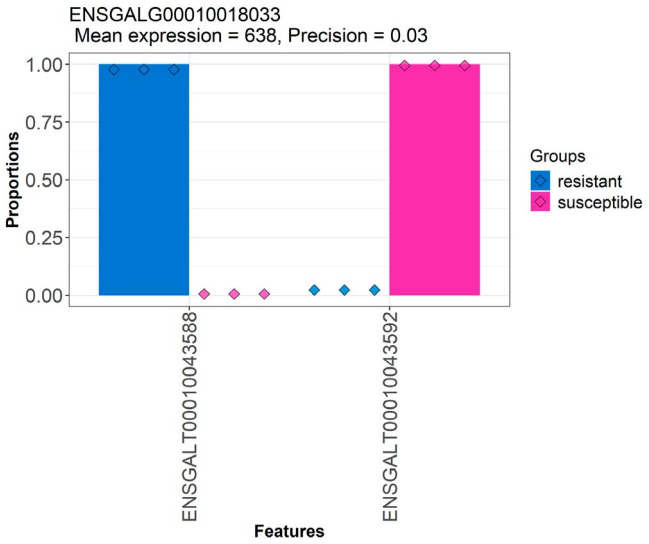

Fig. 6. Plot of the estimated transcript proportions for ENSGALG00010018033 (*COQ8A*)

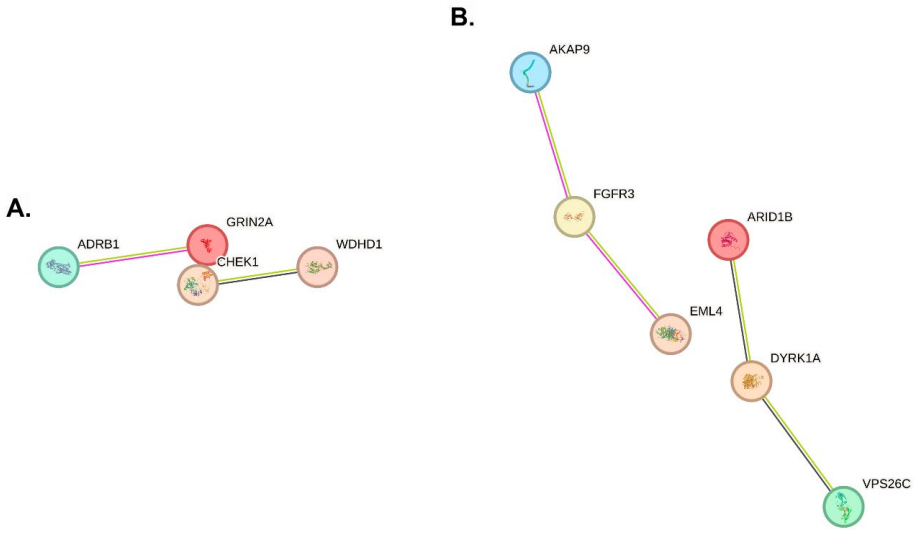

Fig. 7. Interaction analysis of (A) identified differentially expressed genes (B) identified differential transcript usage genes. Disconnected nodes (other DEGs and DTU genes) removed

Discussion

The comparative transcriptomic analysis conducted in this study shows that ALV-J–resistant chickens possess a distinct molecular profile relative to susceptible birds. The consistent separation of samples in clustering analyses, coupled with the large fold changes observed in several differentially expressed genes, indicates substantial biologically meaningful variation between the two phenotypes. This observation aligns with previous transcriptomic investigations showing divergence in gene-expression patterns between ALV-J–positive and uninfected birds (Azamian et al., 2024; Zhang et al., 2025). The additional detection of differential transcript usage (DTU) further supports the idea that alternative splicing contributes to antiviral responses, consistent with findings from Zhang et al. (2025).

A notable feature of the resistant-group expression profile was the strong enrichment of genes associated with mitochondrial biology. Several highly upregulated genes, including *BRAT1, SLC25A43, EARS2*, and *MGM1*, have established links to mitochondrial homeostasis, stress responses, or metabolic regulation. Mitochondria are central to antiviral signaling, particularly through regulation of cytokine production, interferon induction, and apoptosis (Wu et al., 2023). Functional studies indicate that *BRAT1* influences mitochondrial integrity and DNA-damage responses (Aglipay et al., 2006; So and Ouchi, 2014), while *SLC25A43* plays a role in mitochondrial trafficking and cell-cycle control (Gabrielson et al., 2016) and is also implicated as a tumor suppressor (Lindqvist et al., 2012). *EARS2* participates in mitochondrial protein translation (Pelayo et al., 2024), whereas *MGM1* contributes to mitochondrial nucleic-acid metabolism (Yang et al., 2018). Taken together, these findings suggest that enhanced mitochondrial stability and signaling may be an important determinant of ALV-J resistance.

Because mitochondria also serve as hubs for calcium (Ca^{2+}) handling, the enrichment of calcium-signaling genes in resistant birds is notable. Numerous studies highlight the importance of Ca^{2+} flux in modulating viral entry, replication, and host responses (Saurav et al., 2021), and mitochondrial Ca^{2+} balance is known to influence cell fate during infection (Zhou et al., 2009; Chaudhuri et al., 2021). The upregulation of *SMDT1* (*EMRE*), a crucial component of the mitochondrial calcium uniporter (Bulthuis et al., 2023; Wang et al., 2020; Sancak et al., 2013) suggests that ALV-J–resistant chickens may regulate mitochondrial Ca^{2+} uptake more efficiently, potentially contributing to more controlled antiviral responses.

The significance of Ca^{2+} signaling in ALV-J pathogenesis is further supported by the known viral entry mechanism. ALV-J infects host cells through interaction between its Env-J protein and the chicken Na^{+}/H^{+} exchanger 1 (*NHE1*) receptor in a pH-dependent manner (Chai and Bates, 2006). *NHE1* participates in ion transport and has been shown to influence Ca^{2+} regulation in other cell types (Nakamura et al., 2008; Lee et al., 2016). Since *NHE1* is widely expressed across chicken breeds (Mo et al., 2022), variations downstream of receptor signaling – rather than receptor presence itself – may help explain natural resistance.

The upregulation of *CASR*, a calcium-sensing receptor, in resistant birds further reinforces the role of Ca^{2+}-dependent pathways. *CASR* modulates cellular calcium influx and has been shown to suppress replication of rotavirus, demonstrating antiviral potential (Huang et al., 2022). It is plausible that similar mechanisms influence ALV-J outcomes.

Beyond mitochondrial and Ca^{2+} pathways, several genes associated with tumor suppression, DNA-damage checkpoint integrity, and proliferation control were also upregulated in resistant chickens. These include *MTMR7, CHEK1, CKB, CINP*, and others. *MTMR7* expression is reduced in colorectal cancer and has tumor-suppressive activity (Weidner et al., 2016; Weidner et al., 2024). *CHEK1* supports DNA-damage signaling via ATM/ATR pathways (Jiang et al., 2024; Fernandez et al., 2025) and is known to be downregulated by certain viral infections (Akgül et al., 2019). *CKB* inhibits AKT activation and suppresses tumor progression (Wang et al., 2021). *CINP* is critical for ATR-mediated replication stress responses (Lovejoy et al., 2009). The induction of these genes in resistant birds suggests a cellular environment that more effectively limits uncontrolled proliferation, which is a relevant observation given ALV-J's oncogenic properties.

Additionally, several immune-regulatory genes, including *ZNF341, GAB3, LRAT*, and *TMEM104*, were elevated in resistant chickens. *ZNF341* regulates *STAT3*, a central mediator of immune homeostasis (Cekic et al., 2022; Frey-Jakobs et al., 2018). *GAB3* participates in immune-cell signaling (Vaughan et al., 2011) and is linked to malignancy in certain contexts (Jia et al., 2017). *LRAT* is central to vitamin A metabolism, which is tightly connected to antiviral immunity (McGill et al., 2019; Zhang et al., 2023; Stephensen and Lietz, 2021). *TMEM104*, previously shown to be downregulated through promoter methylation in ALV-J–positive chickens (Yan et al., 2021), was upregulated in the resistant group, supporting its potential protective role.

DTU analysis expanded these observations by identifying isoform-level differences in genes implicated in tumor suppression, signaling, and mitochondrial dynamics, such as *ARID1B, HIC2, RIT1, MCT1, MAGI1*, and *GABARAPL1*. These findings correspond with previous reports of isoform dysregulation in cancer and viral infections (Deogharkar et al., 2021; Luo et al., 2023; Khalil and Nemer 2020; de Carvalho et al., 2021; Lake et al., 2013). Notably, *GABARAPL1* is associated

with autophagy, mitochondrial quality control, and resistance to ferroptosis (Boyer-Guittaut et al., 2014; Du et al., 2022), all of which are features that could influence ALV-J disease progression.

While the results seem promising, some limitations are observed. The sample sizes are small which may limit the generalizability of the results identified. Also, results of this study require validation in larger sample groups and other animal cohorts. This will illuminate and validate the results obtained in this study and strengthen the potential role of the genes identified as biomarkers.

Taken together, these results indicate that ALV-J resistance potentially arises from coordinated regulation of several biological systems, including mitochondrial function, Ca^{2+} signaling, immune modulation, and cell-cycle control. The concurrent involvement of DGE and DTU mechanisms suggests that both transcriptional and post-transcriptional processes help shape the resistant phenotype. These findings provide a robust foundation for future functional validation studies and highlight several genes that may serve as biomarkers for breeding programs aimed at enhancing resistance to ALV-J.

Conclusion

This study provides new insight into the molecular features that distinguish ALV-J-resistant chickens from susceptible ones. By integrating differential gene expression, isoform-level analysis, and protein–protein interaction modelling, we identified a set of genes and pathways that may characterize the resistant phenotype. These include regulators of mitochondrial integrity, calcium signaling, immune modulation, and cell-cycle control, systems that collectively influence how host tissues respond to viral challenges.

The presence of strong transcriptomic differences, together with pronounced alternative transcript usage, suggests that resistance is shaped by both transcriptional and post-transcriptional mechanisms. Several of the genes highlighted here may represent promising markers for future validation studies and may have practical value in selective breeding programs aimed at reducing flock susceptibility to ALV-J.

Overall, the findings broaden our understanding of the biological basis of natural resistance and establish a framework for exploring functional mechanisms that contribute to improved disease outcomes. Further experimental work will be essential to confirm the specific roles of these candidate genes and to determine how they can be effectively incorporated into long-term control and breeding strategies.

Acknowledgements

The authors acknowledge the FAANG project for providing open-access RNA-Seq datasets. No external funding was received for this study.

References

1. Aglipay, J.A., Martin, S.A., Tawara, H., Lee, S.W. and Ouchi, T. *ATM* activation by ionizing radiation requires *BRCA1*-associated *BAAT1*. Journal of Biological Chemistry. 2006. 281. 14. P. 9710-–9718.
2. Akgül, B., Kirschberg, M., Storey, A. and Hufbauer, M. Human papillomavirus type 8 oncoproteins E6 and E7 cooperate in downregulation of the cellular checkpoint kinase-1. International Journal of Cancer. 2019. 145. 3. P. 797–806.
3. Anders, S., Reyes, A. and Huber, W. Detecting differential usage of exons from RNA-seq data. Genome Research. 2012. 22. 10. P. 2008–2017.
4. Azamian, P., Foroutanifar, S. and Abdolmohammadi, A. Transcriptomic analysis of host immune response in the chickens infected by avian leukosis virus J using RNA-Seq. Journal of Poultry Sciences and Avian Diseases. 2024. 2. 3. P. 29–39.
5. Bolger, A.M., Lohse, M. and Usadel, B. Trimmomatic: a flexible trimmer for Illumina sequence data. Bioinformatics. 2014. 30. 15. P. 2114–2120.
6. Boyer-Guittaut, M., Poillet, L., Liang, Q., Bôle-Richard, E., Ouyang, X., Benavides, G.A., Chakrama, F.Z., Fraichard, A., Darley-Usmar, V.M., Despouy, G., Jouvenot, M., Delage-Mourroux, R. and Zhang, J. The role of *GABARAPL1/GEC1* in autophagic flux and mitochondrial quality control in MDA-MB-436 breast cancer cells. Autophagy. 2014. 10. 6. P. 986–1003.
7. Bray, N.L., Pimentel, H., Melsted, P. and Pachter, L. Near-optimal probabilistic RNA-seq quantification. Nature Biotechnology. 2016. 34. 5. P. 525–527.
8. Bulthuis, E.P., Adjobo-Hermans, M.J.W., de Potter, B., Hoogstraten, S., Wezendonk, L.H.T. and Tutakhel, O.A.Z. *SMDT1* variants impair *EMRE*-mediated mitochondrial calcium uptake in patients with muscle involvement. BBA - Molecular Basis of Disease. 2003. 1869. 8. 166808.
9. Cekic, S., Huriyet, H., Hortoglu, M., Kasap, N., Ozen, A., Karakoc-Aydiner, E., Metin, A., Ocakoglu, G., Demiroz Abakay, C., Temel, S.G., Ozemri Sag, S., Baris, S., Cavas, T. and Sebnem Kilic, S. Increased radiosensitivity and impaired DNA repair in patients with STAT3-LOF and ZNF341 deficiency, potentially contributing to malignant transformations. Clinical and Experimental Immunology. 2022. 209. 1. P. 83–89.
10. Chai, N. and Bates, P. Na+/H+ exchanger type 1 is a receptor for pathogenic subgroup J avian leukosis virus. Proceedings of the National Academy of Sciences of the United States of America. 2006. 103. P. 5531–5536.
11. Chaudhuri, R., Arora, H. and Seth, P. Mitochondrial calcium signaling in the brain and its modulation by neurotropic viruses. Mitochondrion. 2021. 59. P. 8–16.
12. de Carvalho, P.A., Bonatelli, M., Cordeiro, M.D., Coelho, R.F., Reis, S., Srougi, M., Nahas, W.C., Pinheiro, C. and Leite, K.R.M. *MCT1* expression is independently related to shorter cancer-specific survival in clear cell renal cell carcinoma. Carcinogenesis. 2021. 42. 12. P. 1420–1427.
13. Deogharkar, A., Singh, S.V., Bharambe, H.S., Paul, R., Moiyadi, A., Goel, A., Shetty, P., Sridhar, E., Gupta, T., Jalali, R., Goel, N., Gadewal, N., Muthukumar, S. and Shirsat, N.V. Downregulation of *ARID1B*, a tumor suppressor in the WNT subgroup medulloblastoma, activates multiple oncogenic signaling pathways. Human Molecular Genetics. 2021. 30. 18. P. 1721–1733.
14. Du, X., Qi, Z., Xu, J., Guo, M., Zhang, X., Yu, Z., Cao, X. and Xia, J. Loss of *GABARAPL1* confers ferroptosis resistance to cancer stem-like cells in hepatocellular carcinoma. Molecular Oncology. 2022. 16. 20. P. 3703-3719.
15. Fernandez, A., Artola, M., Leon, S., Otegui, N., Jimeno, A., Serrano, D. and Calvo, A. Cancer vulnerabilities through targeting the ATR/Chk1 and ATM/Chk2 axes in the context of DNA damage. Cells. 2025. 14. 748.
16. Frey-Jakobs, S., Hartberger, J.M., Fliegauf, M., Bossen, C., Wehmeyer, M.L. and Neubauer, J.C. *ZNF341* controls *STAT3* expression and thereby immunocompetence. Science Immunology. 2018. 3. 24. 4941.

17. Gabrielson, M., Reizer, E., Stål, O. and Tina, E. Mitochondrial regulation of cell cycle progression through *SLC25A43*. Biochemical and Biophysical Research Communications. 2016. 469. 4. P. 1090–1096.
18. Han, X., Pan, Y., Shen, Z., Zhang, W. and Jiang, Y. Genome-wide analysis of differential gene expression in response to avian leukosis virus subgroup J infection in chickens. Gene. 2015. 555. 2. P. 294–301.
19. Han, H., Cho, J.W., Lee, S., Yun, A., Kim, H., Bae, D., Yang, S., Kim, C.Y., Lee, M., Kim, E., Lee, S., Kang, B., Jeong, D., Kim, Y., Jeon, H.N., Jung, H., Nam, S., Chung, M., Kim, J.H. and Lee, I. TRRUST v2: an expanded reference database of human and mouse transcriptional regulatory interactions. Nucleic Acids Research. 2018. 46. D1. P. D380-D386.
20. Huang, H., Liao, D., He, B., Cui, Y., Pu, R. and Zhou, G. Calcium-sensing receptor acts as an antiviral factor for rotavirus infections and participates in cellular antiviral response. Iranian Journal of Basic Medical Sciences. 2022. 25. P. 997–1001.
21. Jia, P., Li, F., Gu, W., Zhang, W. and Cai, Y. Gab3 overexpression in human glioma mediates Akt activation and tumor cell proliferation. PLoS One. 2017. 12. 3. e0173473.
22. Jiang, K., Deng, M., Du, W., Liu, T., Li, J. and Zhou, Y. Functions and inhibitors of *CHK1* in cancer therapy. Medicine in Drug Discovery. 2024. 22. 100185.
23. Justice, J. 4th, Malhotra, S., Ruano, M., Li, Y., Zavala, G., Lee, N., Morgan, R. and Beemon, K. The MET gene is a common integration target in avian leukosis virus subgroup J-induced chicken hemangiomas. Journal of Virology. 2015. 89. 9. P. 4712–4719.
24. Khalil, A. and Nemer, G. The potential oncogenic role of the RAS-like GTP-binding gene *RIT1* in glioblastoma. Cancer Biomarkers. 2020. 29. P. 509–519.
25. Lake, S.L., Damato, B.E., Kalirai, H., Dodson, A.R., Taktak, A.F., Lloyd, B.H. and Coupland, S.E. Single nucleotide polymorphism array analysis of uveal melanomas reveals that amplification of *CNKSR3* is correlated with improved patient survival. American Journal of Pathology. 2013. 182. 3. P. 678–87.
26. Lee, H.C., Yoon, S.Y., Lykke-Hartmann, K., Fissore, R.A. and Carvacho, I. *TRPV3* channels mediate Ca^{2+} influx induced by 2-APB in mouse eggs. Cell Calcium. 2016. 59. 1. P. 21–31.
27. Lindqvist, B.M., Farkas, S.A., Wingren, S. and Nilsson, T.K. DNA methylation pattern of the *SLC25A43* gene in breast cancer. Epigenetics. 2012. 7. 3. P. 300–306.
28. Love, M.I., Huber, W. and Anders, S. Moderated estimation of fold change and dispersion for RNA-seq data with DE-Seq2. Genome Biology. 2014. 15. 12. 550.
29. Love, M.I., Soneson, C. and Patro, R. Swimming downstream: statistical analysis of differential transcript usage following Salmon quantification. F1000Research. 2018. 7. 952.
30. Lovejoy, C.A., Xu, X., Bansbach, C.E., Glick, G.G., Zhao, R., Ye, F., Sirbu, B.M., Titus, L.C., Shyr, Y. and Cortez, D. Functional genomic screens identify *CINP* as a genome maintenance protein. Proceedings of the National Academy of Sciences of the United States of America. 2009. 106. 46. P. 19304–19309.
31. Luo, F., Liao, Y., Cao, E., Yang, Y., Tang, K., Zhou, D., Zhou, D. and Cai, H. Hypermethylation of *HIC2* is a potential prognostic biomarker and tumor suppressor of glioma based on bioinformatics analysis and experiments. CNS Neuroscience & Therapeutics. 2023. 29. 4. P. 1154–1167.
32. McGill, J.L., Kelly, S.M., Guerra-Maupome, M., Winkley, E., Henningson, J., Narasimhan, B. and Sacco, R.E. Vitamin A deficiency impairs the immune response to intranasal vaccination and RSV infection in neonatal calves. Scientific Reports. 2019. 9. 15157.
33. Mo, G., Wei, P., Hu, B., Nie, Q. and Zhang, X. Advances on genetic and genomic studies of ALV resistance. Journal of Animal Science and Biotechnology. 2022. 13. 1. 123.
34. Nakamura, K., Kamouchi, M., Kitazono, T., Kuroda, J., Matsuo, R., Hagiwara, N., Ishikawa, E., Ooboshi, H., Ibayashi, S. and Iida, M. Role of *NHE1* in calcium signaling and cell proliferation in human CNS pericytes. American Journal of Physiology – Heart and Circulatory Physiology. 2008. 294. P. H1700–H1707.
35. Nakamura, L.P. and Nair, V. The long view: 40 years of avian leukosis research. Avian Pathology. 2014. 41. 1. P. 11–19.
36. Nowicka, M. and Robinson, M.D. DRIMSeq: a Dirichlet-multinomial framework for multivariate count outcomes in genomics. F1000 Research. 2016. 5. 1356.
37. Payne, L.N. and Nair, V. The long view: 40 years of avian leukosis research. Avian Pathology. 2012. 41. 1. P. 11–19.
38. Pelayo, G., Paiva Coelho, M., Correia, J., Bandeira, A., Nogueira, C., Vilarinho, L. and Martins, E. Phenotyping mitochondrial glutamyl-tRNA synthetase deficiency (*EARS2*): A case series and systematic literature review. Neurobiology of Disease. 2024. 200. 106644.
39. Raun, S.B., Salter, D.W. and Burton, R.S. Transcriptome profiling and the study of gene expression: techniques and applications in animal biology. Journal of Animal Science. 2004. 82. P. E66–E76.
40. Ren, C., Yu, M., Zhang, Y., Fan, M., Chang, F., Xing, L., Liu, Y., Wang, Y., Qi, X., Liu, C., Zhang, Y., Cui, H., Li, K., Gao, L., Pan, Q., Wang, X. and Gao, Y. Avian leukosis virus subgroup J promotes cell proliferation and cell cycle progression through miR-221 by targeting CDKN1B. Virology. 2018. 519. P. 121–130.
41. Reyes, A., Anders, S., Weatheritt, R.J., Gibson, T.J., Steinmetz, L.M. and Huber, W. Drift and conservation of differential exon usage across tissues in primate species. Proceedings of the National Academy of Sciences of the United States of America. 2013. 110. 38. P. 15377–15382.
42. Sancak, Y., Markhard, A.L., Kitami, T., Kovács-Bogdán, E., Kamer, K.J., Udeshi, N.D., Carr, S.A., Chaudhuri, D., Clapham, D.E., Li, A.A., Calvo, S.E., Goldberger, O. and Mootha, V.K. *EMRE* is an essential component of the mitochondrial calcium uniporter complex. Science. 2013. 342. 6164. P. 1379–1382.
43. Saurav, S., Tanwar, J., Ahuja, K. and Motiani, R.K. Dysregulation of host cell calcium signaling during viral infections: Emerging paradigm with high clinical relevance. Molecular Aspects of Medicine. 2021. 81. 101004.
44. So, E.Y. and Ouchi, T. *BRAT1* deficiency causes increased glucose metabolism and mitochondrial malfunction. BMC Cancer. 2014. 14. 548.
45. Soneson, C., Love, M.I. and Robinson, M.D. Differential analyses for RNA-seq: transcript-level estimates improve gene-level inferences. F1000Research. 2015. 4. 1521.
46. Stephensen, C.B. and Lietz, G. Vitamin A in resistance to and recovery from infection: relevance to SARS-CoV2. British Journal of Nutrition. 2021. 126. 11. P. 1663–1672.
47. Szklarczyk, D., Gable, A.L., Nastou, K.C., Lyon, D., Kirsch, R., Pyysalo, S., Doncheva, N.T., Legeay, M., Fang, T., Bork, P., Jensen, L.J. and von Mering, C. The STRING database in 2021: customizable protein-protein networks, and functional characterization of user uploaded gene/measurement sets. Nucleic Acids Research. 2021. 49. D1. P. D605–D612.
48. Van den Berge, K., Soneson, C., Robinson, M.D. and Clement, L. stageR: a general stage-wise method for controlling the gene-level false discovery rate in differential expression and differential transcript usage. Genome Biology. 2018. 18. 1. 151.
49. Vaughan, T.Y., Verma, S. and Bunting, K.D. Grb2-associated binding (Gab) proteins in hematopoietic and immune cell biology. American Journal of Blood Research. 2011. 1. 2. P. 130-134.
50. Wang, Y., Han, Y., She, J., Nguyen, N.X., Mootha, V.K., Bai, X.C. and Jiang, Y. Structural insights into the Ca^{2+}-dependent gating of the human mitochondrial calcium uniporter. Elife. 2020. 9. e60513.
51. Wang, Z., Hulsurkar, M., Zhuo, L., Xu, J., Yang, H., Naderinezhad, S., Wang, L., Zhang, G., Ai, N., Li, L., Chang, J.T., Zhang, S., Fazli, L., Creighton, C.J., Bai, F., Ittmann, M.M., Gleave, M.E. and Li, W. CKB inhibits epithelial-mesenchymal transition and prostate cancer progression by sequestering and inhibiting AKT activation. Neoplasia. 2021. 23. 11. P. 1147–1165.
52. Weidner, P., Saar, D., Söhn, M., Schroeder, T., Yu, Y. and Zöllner, F.G. Myotubularin-related-protein-7 inhibits mutant (G12V) K-RAS by direct interaction. Cancer Letters. 2024. 588. 216783.

53. Weidner, P., Söhn, M., Gutting, T., Friedrich, T., Gaiser, T., Magdeburg, J., Kienle, P., Ruh, H., Hopf, C., Behrens, H.M., Röcken, C., Hanoch, T., Seger, R., Ebert, M.P. and Burgermeister, E. Myotubularin-related protein 7 inhibits insulin signaling in colorectal cancer. Oncotarget. 2016. 7. 31. P. 50490-50506.
54. Wessi, J. Avian leukosis virus: Classification, biology, and impact on poultry health. Veterinary Microbiology. 2011. 49. 3. P. 205-214.
55. Wu, M., Pei, Z., Long, G., Chen, H., Jia, Z. and Xia, W. Mitochondrial antiviral signaling protein: a potential therapeutic target in renal disease. Frontiers in Immunology. 2023. 14. 1266461.
56. Yan, Y., Zhang, H., Gao, S., Zhang, H., Zhang, X., Chen, W., Lin, W. and Xie, Q. Differential DNA methylation and gene expression between ALV-J-Positive and ALV-J-Negative chickens. Frontiers in Veterinary Science. 2021. 8. 659840.
57. Yang, C., Wu, R., Liu, H., Chen, Y., Gao, Y., Chen, X., Li, Y., Ma, J., Li, J. and Gan, J. Structural insights into DNA degradation by human mitochondrial nuclease MGME1. Nucleic Acids Research. 2018. 46. 20. P. 11075–11088.
58. Zhang, L., Hou, Y., Ma, Z., Xie, J., Fan, J., Jiao, Y., Wang, F., Han, Z., Liu, S. and Ma, D. Effect of oral vitamin A supplementation on host immune response to infectious bronchitis virus infection in specific pathogen-free chicken. Poultry Science. 2023. 102. 7. 102701.
59. Zhang, Y., Gao, Y., Miao, X., Qu, L. and Ning, Z. Gene expression and alternative splicing reveal the co-regulation of host response mechanisms to avian leukosis virus subgroup J-infected in laying hens. Poultry Science. 2025. 104. 10. 105554.
60. Zhou, Y., Frey, T.K. and Yang, J.J. Viral calciomics: interplays between Ca2+ and virus. Cell Calcium. 2009. 46. P. 1–17.